

The Relationship between NMR Chemical Shifts of Thermally Polarized and Hyperpolarized ^{89}Y Complexes and Their Solution Structures

Yixun Xing^a, Ashish K. Jindal^b, Martín Regueiro-Figueroa^c, Mariane Le Fur^d, Nelly Kervarec^e, Piyu Zhao^a, Zoltan Kovacs^b, Laura Valencia^f, Paulo Pérez-Lourido^f, Raphaël Tripiet^d, David Esteban-Gómez^c, Carlos Platas-Iglesias^c, and A. Dean Sherry^{a,b}

^a Department of Chemistry, University of Texas, Dallas, Richardson, Texas, USA

^b Advanced Imaging Research Center, University of Texas Southwestern Medical Center, Dallas, Texas, USA

^c Centro de Investigaciones Científicas Avanzadas (CICA) y Departamento de Química Fundamental, Facultad de Ciencias, Universidade da Coruña, A Coruña, Galicia, Spain

^d Université de Bretagne Occidentale, UMR-CNRS 6521, UFR des Sciences et Techniques, Brest Cedex 3, France

^e Plateforme de RMN-RPE, Université de Bretagne Occidentale, UMR-CNRS 6521, UFR des Sciences et Techniques, Brest Cedex 3, France

^f Departamento de Química Inorgánica, Facultad de Ciencias, Universidade de Vigo, Pontevedra, Spain

Chemistry - A European Journal Volume 22, Issue 46, pages 16657–16667, November 7, 2016

Issue online: 2 November 2016, Version of record online: 10 October 2016, Manuscript Received: 17 June 2016

This is the peer reviewed version of the following article:

Xing, Y., Jindal, A. K., Regueiro-Figueroa, M., Le Fur, M., Kervarec, N., Zhao, P., Kovacs, Z., Valencia, L., Pérez-Lourido, P., Tripiet, R., Esteban-Gómez, D., Platas-Iglesias, C., Sherry, A. D. (2016), The Relationship between NMR Chemical Shifts of Thermally Polarized and Hyperpolarized ^{89}Y Complexes and Their Solution Structures. *Chem. Eur. J.*, 21: 16657–16667.

which has been published in final form at <https://doi.org/10.1002/chem.201602901>. This article may be used for non-commercial purposes in accordance with Wiley Terms and Conditions for Self-Archiving.

Abstract

Recently developed dynamic nuclear polarization (DNP) technology offers the potential of increasing the NMR sensitivity of even rare nuclei for biological imaging applications. Hyperpolarized ^{89}Y is an ideal candidate because of its narrow NMR linewidth, favorable spin quantum number ($I=1/2$), and long longitudinal relaxation times (T_1). Strong NMR signals were detected in hyperpolarized ^{89}Y samples of a variety of yttrium complexes. A dataset of ^{89}Y NMR data composed of 23 complexes with polyaminocarboxylate ligands was obtained using hyperpolarized ^{89}Y measurements or ^1H , ^{89}Y -HMQC spectroscopy. These data were used to derive an empirical equation that describes the correlation between the ^{89}Y chemical shift and the chemical structure of the complexes. This empirical correlation serves as a guide for the design of ^{89}Y sensors. Relativistic (DKH2) DFT calculations were found to predict the experimental ^{89}Y chemical shifts to a rather good accuracy.

Keywords: density functional calculations; hyperpolarization; magnetic resonance imaging; NMR spectroscopy; yttrium

Introduction

Magnetic resonance imaging (MRI) is a technique widely used in medical diagnosis that is based on the same fundamental principles as NMR spectroscopy. Traditional MRI scanners detect the NMR signal of water proton nuclei present in the body, with image contrast being achieved by using adequate pulse sequences that take advantage of differences in proton densities and longitudinal and transverse relaxation times among tissues.^[1] MRI provides 3D images of the body with very high resolution, but it is traditionally regarded as a rather insensitive technique.^[2] In an external magnetic field B_0 , the extent to which a nuclear spin becomes polarized is described by:^[3]

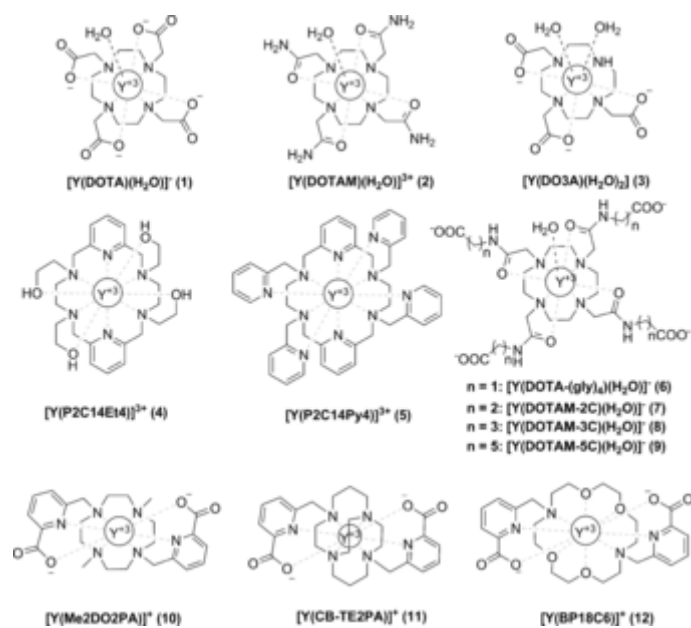
$$P = \frac{(N^+ - N^-)}{(N^+ + N^-)} \quad (1)$$

where N^+ and N^- denote the number of nuclear spins parallel (spin up) and anti-parallel (spin down) with respect to B_0 . The polarization at Boltzmann equilibrium (P_0) is given by:^[4]

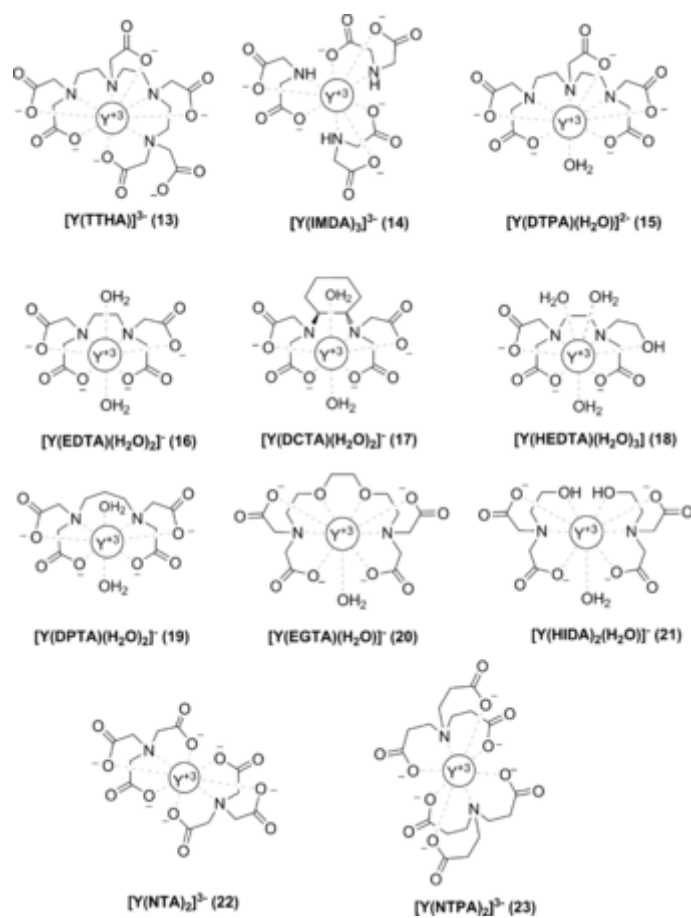
$$P_0 = \tanh\left(\frac{\gamma h B_0}{2k_B T}\right) \approx \frac{\gamma h B_0}{2k_B T} \quad (2)$$

where γ is the gyromagnetic ratio of the nucleus under study, k_B is the Boltzmann constant, and other symbols have their usual meaning. Equation (2) shows that spin polarization increases with field, so the tendency has been for human MRI scanners to move to higher fields over the years to gain sensitivity. Eventually, this becomes cost-prohibitive, so alternative ways to increase NMR sensitivity are being explored. One method is to use hyperpolarized (HP) materials that exist, at least temporarily, in a non-equilibrium hyperpolarized state where $(N^+ - N^-)$ is increased several orders of magnitude over thermal equilibrium. Dynamic nuclear polarization (DNP), one of the more popular methods to produce hyperpolarized materials, has been used to amplify the sensitivity of ^{13}C and ^{15}N nuclei to a level where common metabolites can be imaged by MRI. For example, ^{13}C polarization levels as high as 50% have been achieved using DNP at low temperatures and high fields.^[5] The experimental method involves doping the ^{13}C material with a stable free radical such as trityl or nitroxide, freezing the sample in a solvent that forms a glass, and irradiating the sample with continuous microwave irradiation at a frequency close to the corresponding electron resonance frequency.

Recently we reported the use of DNP methods to hyperpolarize a variety of ^{89}Y complexes.^[6-9] In nature, yttrium exists 100% as the stable isotope ^{89}Y . The predominant chemical form of yttrium is the diamagnetic, trivalent ion, Y^{3+} . ^{89}Y has a much smaller nuclear magnetic moment than ^{13}C , so its NMR sensitivity is only 0.668 relative to ^{13}C .^[10] Consequently, it is quite difficult and time-consuming to acquire an ^{89}Y NMR spectrum at Boltzmann spin levels except for highly concentrated samples. However, $^{89}\text{Y}^{3+}$ has a nuclear spin quantum number of $I=1/2$ and exhibits narrow NMR linewidths and long longitudinal relaxation times (T_1), so it is an attractive nucleus for hyperpolarization. Furthermore, yttrium is not naturally present in the human body, so there is zero background signal. The effective ionic radius of Y^{3+} (1.019 Å for CN8) is similar to that of Gd^{3+} (1.053 Å),^[11] so any ligand used to complex Gd^{3+} will also form stable complexes with Y^{3+} .^[12, 13] Y^{3+} complexes can be also used as models for investigating the solution behavior of the corresponding paramagnetic lanthanide complexes.^[14]



Scheme 1. Complexes with macrocyclic ligands investigated in this work.



Scheme 2. Complexes with non-macrocyclic ligands investigated in this work.

Only a single ^{89}Y NMR report existed before 1970, which is most likely due to the extremely low NMR sensitivity of this nucleus.^[15] In the late 1970s the first T_1 values for some ^{89}Y complexes were found to be unusually long.^[16] In 2007, three ^{89}Y complexes, Y-DOTP, Y-DOTA, Y-DTPA, along with YCl_3 were hyperpolarized using DNP methods and NMR signals were obtained on complexes at concentrations of only 5–15 mM after a single scan.^[6] The enhanced signals showed that yttrium complexes could be polarized to levels reasonable for imaging. Furthermore, the various ^{89}Y complexes displayed a wide range of chemical shifts. This observation in combination with the long relaxation times of these complexes makes them potentially attractive as probes for various physiological parameters such as pH or redox environment. This preliminary study triggered our interest in conducting hyperpolarization experiments on a broader range of ^{89}Y complexes. We report herein ^{89}Y NMR spectra of both thermally polarized and hyperpolarized samples of the diverse group of Y^{3+} complexes shown in Scheme 1 and Scheme 2. Subsequently, density functional theory (DFT) calculations were conducted to better understand the factors that affect the observed ^{89}Y NMR chemical shifts and eventually establish empirical correlations between NMR chemical shifts and the number and types of donor atoms in each complex, which might serve as a guide for designing new ^{89}Y complexes as biosensors.

Results and Discussion

Structure of the Y^{3+} complexes

Establishing a correlation between the observed ^{89}Y NMR chemical shifts and the coordination environment around the metal ion requires an accurate determination of the structure of the concerned complexes in solution. Given the similar coordination properties of Y^{3+} and the lanthanide ions (Ln^{3+}) we sought to expand the family of structurally characterized Y^{3+} complexes by taking advantage of our recent studies on Ln^{3+} complexes. Thus, we have included in our studies a series of macrocyclic-based ligand complexes, $[\text{Y}(\text{Me}_2\text{DO}_2\text{PA})]^+$, $[\text{Y}(\text{CB-TE}_2\text{PA})]^+$, $[\text{Y}(\text{P}2\text{C}14\text{Et}4)]^{3+}$, $[\text{Y}(\text{P}2\text{C}14\text{Py}4)]^{3+}$, and $[\text{Y}(\text{BP}18\text{C}6)]^+$ (Scheme 1), where the structures of the corresponding Ln^{3+} complexes have been established by X-ray diffraction in the solid state and/or by analysis of the Ln^{3+} -induced paramagnetic ^1H NMR shifts in aqueous solution.^[17-25] The X-ray structure obtained using single crystals with formula $[\text{Y}(\text{P}2\text{C}14\text{Et}4)](\text{NO}_3)_3 \cdot 6\text{H}_2\text{O}$ confirm that the $[\text{Y}(\text{P}2\text{C}14\text{Et}4)]^{3+}$ complex retains the ten-coordinate structure observed for the Ln^{3+} series along the whole lanthanide series (Figure 1).^[20, 25] Similarly, the $[\text{Y}(\text{Me}_2\text{DO}_2\text{PA})]^+$ and $[\text{Y}(\text{CB-TE}_2\text{PA})]^+$ complexes adopt eight-coordinate structures in the solid state very similar to those established for the corresponding complexes with the Ln^{3+} ions (Figure 2 and Figure 3).^[18, 19, 21] The family of Y^{3+} complexes with macrocyclic ligands investigated in this work also includes $[\text{Y}(\text{DOTA})(\text{H}_2\text{O})]^-$, $[\text{Y}(\text{DOTAM})(\text{H}_2\text{O})]^{3+}$ and $[\text{Y}(\text{DO}_3\text{A})(\text{H}_2\text{O})_2]^-$. The structure of $[\text{Y}(\text{DOTA})(\text{H}_2\text{O})]^-$ in the solid state has been established by X-ray diffraction,^[26, 27] while the structure of Ln^{3+} complexes of these ligands have been also investigated both in the solid state and in solution.^[28-33] The Gd^{3+} complex of DO3A was shown to be present in solution as a hydration equilibrium involving an eight-coordinated $[\text{Gd}(\text{DO}_3\text{A})(\text{H}_2\text{O})]$ complex and a nine-coordinated bis-hydrated $[\text{Gd}(\text{DO}_3\text{A})(\text{H}_2\text{O})_2]$ complex. The speciation in solution was found to be dominated by the bis-hydrated form, which results in an overall hydration number of 1.8–1.9 at 25 °C.^[34, 35]

The chemical formula of all Y^{3+} complexes with non-macrocyclic ligands included in this study are shown in Scheme 2. The number of inner-sphere water molecules in some of the complexes was assigned on the basis of available crystallographic data and solution studies performed on the Ln^{3+} analogues ($[\text{Y}(\text{EGTA})(\text{H}_2\text{O})]^-$,^[36, 37] $[\text{Y}(\text{DTPA})(\text{H}_2\text{O})]^{2-}$,^[38] $[\text{Y}(\text{TTHA})]^{3-}$ ^[39]). In other cases the complexes present variable hydration numbers in the solid state so the exact number of water molecules coordinated to Y^{3+} cannot be predicted in a straightforward manner. For instance, the sodium salt of $[\text{Y}(\text{EDTA})(\text{H}_2\text{O})_3]^-$ was found to contain three coordinated water molecules, while the structurally related $[\text{Y}(\text{DCTA})(\text{H}_2\text{O})_2]^-$ complex was reported to be bis-hydrated in the solid state.^[40] The number of coordinated

water molecules in these complexes was assessed by using DFT calculations, which provided theoretical ^{89}Y NMR shifts using different plausible coordination numbers. The comparison of experimental and calculated shifts allowed an unequivocal assignment of the hydration state (see below). Most ligands included in this study are known to form 1:1 complexes with the trivalent Ln^{3+} ions, except for NTA^{3-} and NTPA^{3-} , which can form both 1:1 and 1:2 complexes, or HIDA^{2-} and IMDA^{2-} , which form 1:2 and 1:3 complexes, respectively.^[10]

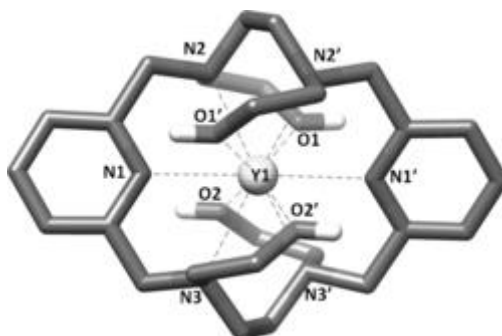


Figure 1. View of one of the complex cations present in crystals of $[\text{Y}(\text{P2C14Et4})](\text{NO}_3)_3 \cdot 6\text{H}_2\text{O}$. Water molecules, anions and hydrogen atoms (except those of the hydroxy groups) have been omitted for simplicity. Bond distances [\AA]: Y1–O1 2.435(2), Y1–O2 2.442(2), Y1–N1 2.562(2), Y1–N2 2.628(3), Y1–N3 2.657(3).

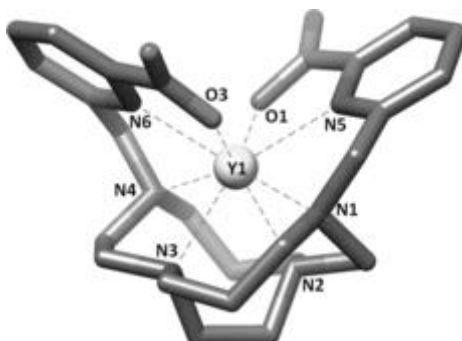


Figure 2. View of one of the complex cations present in crystals of $[\text{Y}(\text{CB-TE2PA})](\text{PF}_6)_2 \cdot 2.5\text{H}_2\text{O}$. Water molecules, anions and hydrogen atoms have been omitted for simplicity. Bond distances [\AA]: Y1–O1 2.275(4), Y1–O3 2.259(4), Y1–N1 2.590(5), Y1–N2 2.526(5), Y1–N3 2.607(5), Y1–N4 2.520(4) Y1–N5 2.459(5), Y1–N6 2.470(5).

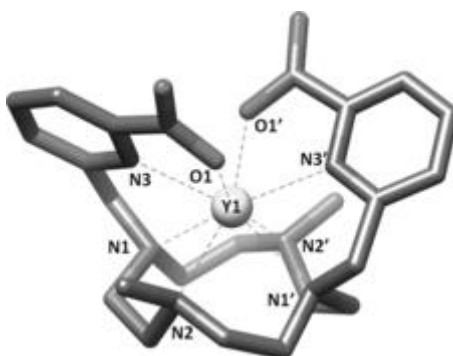


Figure 3. View of one of the complex cations present in crystals of $[\text{Y}(\text{Me}_2\text{DO}_2\text{PA})](\text{PF}_6)_2 \cdot 2\text{H}_2\text{O}$. Water molecules, anions, and hydrogen atoms have been omitted for simplicity. Bond distances [\AA]: Y1–O1 2.272(2), Y1–N1 2.565(2), Y1–N2 2.569(3), Y1–N3 2.425(2). The complex presents a crystallographically imposed C_2 symmetry.

^{89}Y NMR chemical shifts

^{89}Y NMR spectra of hyperpolarized samples of Y^{3+} -EDTA and Y^{3+} -EGTA are illustrated in Figure 4. These spectra demonstrate that one can obtain high-quality ^{89}Y NMR spectra relatively easily. The ^{89}Y chemical shifts of seven complexes measured on hyperpolarized samples are listed in Table 1. Thermally polarized ^{89}Y spectra have been reported previously for Y^{3+} -(DTPA), Y^{3+} -EGTA, Y^{3+} -(NTA)₂, Y^{3+} -EDTA, and Y^{3+} -TTHA, and their chemical shifts agree well with those measured from spectra of hyperpolarized samples.^[10, 41]

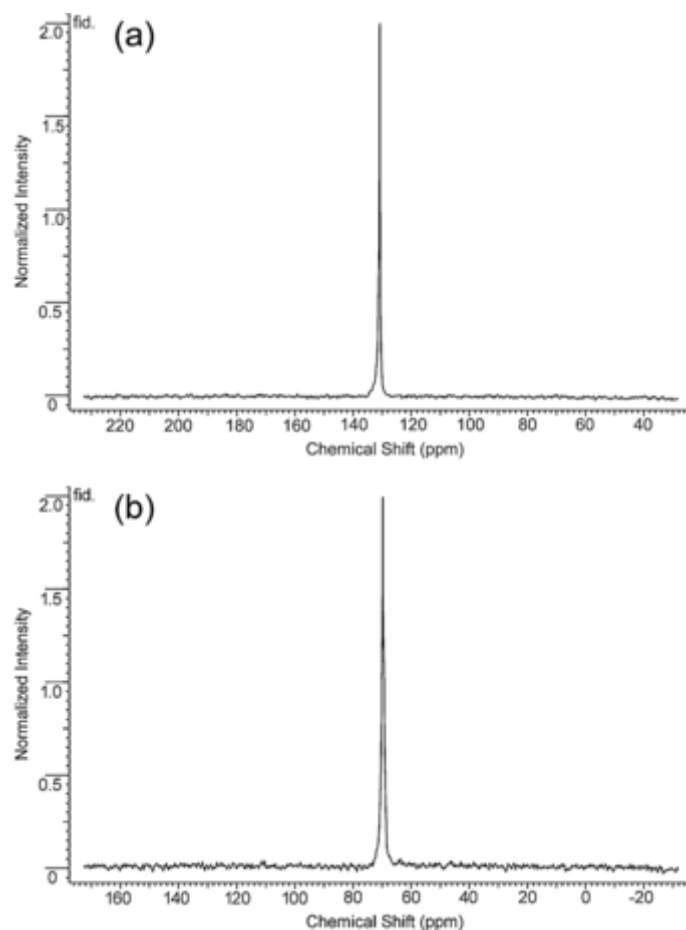


Figure 4. NMR spectra of hyperpolarized a) Y^{3+} -EDTA (6.1 mM) and b) Y^{3+} -EGTA (7.7 mM) at pH 7.4 collected at 9.4 T using a single 20° pulse.

Another set of ^{89}Y NMR shifts was obtained using ^1H , ^{89}Y heteronuclear shift correlation through scalar coupling (^1H , ^{89}Y -HMQC). This technique allows a much faster acquisition compared with conventional pulse-acquisition ^{89}Y NMR measurements, which are very time-consuming owing to the long T_1 relaxation times of ^{89}Y (Table 1). ^1H , ^{89}Y -HMQC spectroscopy allows an indirect ^1H detection of ^{89}Y , thereby overcoming this problem.^[42] The representative example of the ^1H , ^{89}Y -HMQC spectrum of $[\text{Y}(\text{P2C14Et4})]^{3+}$ is shown in Figure 5. Several cross-peaks relating the ^{89}Y NMR signal of the complex at 25.7 ppm and aliphatic protons of the ligand situated at a three-bond distance are observed. A weak correlation involving the pyridyl proton H2, situated four bonds away the metal ion, is also evident. The strongest correlations involve H4_{ax}, H5_{ax}, H7_{eq}, and H7_{ax}, which according to the X-ray crystal structure present H-C-N-Y or H-C-O-Y dihedral angles of 80.6, 78.4, 104.1, and 136.9°. However, no cross-peaks are observed in the case of protons H4_{eq} and H5_{eq}, which are characterized by dihedral angles of 162.2 and 163.5°. These results suggest that the intensity of the scalar coupling between ^1H and ^{89}Y follows a Karplus-like

relationship, as observed for the ^1H scalar coupling constants responsible for the contact shifts induced by paramagnetic Ln^{3+} ions.^[19]

Table 1. ^{89}Y chemical shifts and T_1 values for seven hyperpolarized Y^{3+} complexes.^[a]

Y^{3+} complex	Concentration [mM]	Chemical shift [ppm]	T_1 [s]
EGTA	7.7	68.6	474±13
(NTA) ₂	7.2	73.0	534±118
DTPA	6.2	76.0	227±5
DO3 A	7.2	103.5	247±91
EDTA	6.1	133.5	310±4
DOTA	12.5	111.3	446±7
TTHA	7.7	96.9	245±90
		103.2	230±14

[a] Circa 0.2 M samples dissolved in H_2O /glycerol (3:1) plus 15 mM OX63 were frozen at 1.4 K and polarized for 3 h in an Oxford DNP HyperSense system. The samples were quickly dissolved in a buffer and transferred to a 10 mm NMR tube for data collection using a 9.4T magnet. ^{89}Y spectra were collected using 20° pulses every 20 s over a period of 300–600 s and the resulting data were fitted to standard decay curve for polarized samples. All chemical shifts are reported relative to YCl_3 set to 0 ppm.

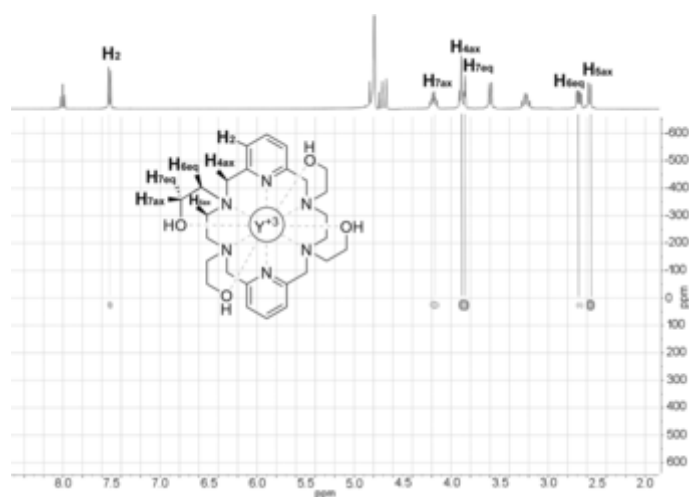


Figure 5. ^1H , ^{89}Y -HMQC NMR spectrum of $[\text{Y}(\text{P}2\text{C}14\text{Et}4)]^{3+}$ recorded in D_2O solution (4.7 mM).

The ^{89}Y NMR chemical shift data of the complexes investigated in this work are compiled in Table 2. The yttrium chemical shifts of our data set composed of 23 polyamino-polycarboxylate complexes vary over 270 ppm. Particularly surprising are the shifts of $[\text{Y}(\text{Me}_2\text{DO}_2\text{PA})]^+$ (245.8 ppm) and $[\text{Y}(\text{CB-TE}_2\text{PA})]^+$ (218.5 ppm) and the negative chemical shift of $[\text{Y}(\text{BP18C6})]^+$ (-23.6 ppm), which expand the ^{89}Y NMR chemical shift range of polyaminocarboxylate complexes by about 200 ppm with respect to the window of ^{89}Y NMR shifts reported previously (ca. 70 ppm).^[10, 41]

Table 2. Measured chemical shifts and predicted chemical shifts from (3) of Y^{3+} complexes with the numbers of coordinated amine nitrogen atoms (n_{Nam}), pyridine nitrogen atoms (n_{Npy}), carboxylate oxygen atoms (n_{Oc}), ether oxygen atoms (n_{Oe}), amide oxygen atoms (n_{Oa}), and water oxygen atoms (n_{Ow}).^[a]

Y^{3+} complex	δ^{exp} (ppm)	δ^{calc} (ppm)	n_{Nam}	n_{Npy}	n_{Oc}	n_{Oe}	n_{Oh}	n_{Oa}	n_{Ow}
$[\text{Y}(\text{DOTA})(\text{H}_2\text{O})]^-$ (1)	111.3	107.0	4	0	4	0	0	0	1
$[\text{Y}(\text{DOTAM})(\text{H}_2\text{O})]^{3+}$ (2)	123.0 ^[b]	125.1	4	0	0	0	0	4	1
$[\text{Y}(\text{DO}_3\text{A})(\text{H}_2\text{O})_2]$ (3)	103.5	93.4	4	0	3	0	0	0	2
$[\text{Y}(\text{P2C14Et}_4)]^{3+}$ (4)	25.7	29.8	4	2	0	0	4	0	0
$[\text{Y}(\text{P2C14Py}_4)]^{3+}$ (5)	78.6	76.0	4	6	0	0	0	0	0
$[\text{Y}(\text{DOTA}-(\text{gly})_4)(\text{H}_2\text{O})]^-$ (6)	121.6	125.1	4	0	0	0	0	4	1
$[\text{Y}(\text{DOTAM}-2\text{C})(\text{H}_2\text{O})]^-$ (7)	120.9	125.1	4	0	0	0	0	4	1
$[\text{Y}(\text{DOTAM}-3\text{C})(\text{H}_2\text{O})]^-$ (8)	118.7	125.1	4	0	0	0	0	4	1
$[\text{Y}(\text{DOTAM}-5\text{C})(\text{H}_2\text{O})]^-$ (9)	117.8	125.1	4	0	0	0	0	4	1
$[\text{Y}(\text{Me}_2\text{DO}_2\text{PA})]^+$ (10)	244.7	231.0	4	0	0	0	0	0	0
$[\text{Y}(\text{CB-TE}_2\text{PA})]^+$ (11)	218.5	231.0	4	0	0	0	0	0	0
$[\text{Y}(\text{BP18C6})]^+$ (12)	-23.6	-15.3	2	0	0	4	0	0	0
$[\text{Y}(\text{TTHA})]^{3-}$ (13)	103.2	120.6	4	0	5	0	0	0	0
$[\text{Y}(\text{IMDA})_3]^{3-}$ (14)	98.7 ^[c]	94.7	3	0	6	0	0	0	0
$[\text{Y}(\text{DTPA})(\text{H}_2\text{O})]^{2-}$ (15)	76.0, 82.2, ^[c] 83.0 ^[d]	81.1	3	0	5	0	0	0	1

Y^{3+} complex	δ^{exp} (ppm)	δ^{calc} (ppm)	n_{Nam}	n_{Npy}	n_{Oc}	n_{Oe}	n_{Oh}	n_{Oa}	n_{Ow}
[Y(EDTA)(H ₂ O) ₂] ⁻ (16)	133.5, 129.6 ^[c]	135.7	2	0	4	0	0	0	2
[Y(DCTA)(H ₂ O) ₂] ⁻ (17)	132.7 ^[c]	135.7	2	0	4	0	0	0	2
[Y(HEDTA)(H ₂ O) ₂] (18)	78.6 ^[c]	76.0	2	0	3	0	1	0	3
[Y(DPTA)(H ₂ O) ₂] ⁻ (19)	130.0 ^[c]	135.7	2	0	4	0	0	0	2
[Y(EGTA)(H ₂ O)] ⁻ (20)	68.6, 69.4, ^[d] 68.5 ^[c]	52.0	2	0	4	2	0	0	1
[Y(HIDA) ₂] ⁻ (21)	57.0 ^[c]	48.6	2	0	4	0	2	0	1
[Y(NTA) ₂] ³⁻ (22)	73.0, 76.5 ^[c]	162.8	2	0	6	0	0	0	0
		55.2	2	0	6	0	0	0	1
[Y(NTPA) ₂] ³⁻ (23)	90.5 ^[c]	162.8	2	0	6	0	0	0	0
		55.2	2	0	6	0	0	0	1
[Y(NTA)] (24)	62.6 ^[c]	82.5	1	0	3	0	0	0	4
		-25.1	1	0	3	0	0	0	5
[Y(NTPA)] (25)	44.0 ^[c]	82.5	1	0	3	0	0	0	4
		-25.1	1	0	3	0	0	0	5
[Y(H ₂ O) ₈] ³⁺ (26)	0.0	2.5	0	0	0	0	0	0	8

[a] $S_{Nam}=68.1\pm 6.4$, $S_{Npy}=85.7\pm 5.4$, $S_{Oc}=94.0\pm 5.8$, $S_{Oe}=95.7\pm 4.9$, $S_{Oh}=97.3\pm 4.9$, $S_{Oa}=89.5\pm 5.4$, $S_{Ow}=107.6\pm 6.2$. [b] Data from Ref. [45]. [c] Data from Ref. [10]. [d] Thermally polarized data (this work).

The sensitivity of the ⁸⁹Y NMR chemical shift to the ligand field produced by the chelate has been examined before for a series of organometallic complexes,^[43] but few studies have attempted to relate ⁸⁹Y chemical shifts with coordination number and identity of donor atoms in ligands that could potentially serve as reporter molecules in biological systems. An empirical relationship between the number of coordinated oxygen and nitrogen atoms and ¹³⁹La chemical shifts was reported previously.^[44] In that study, each negatively charged oxygen atom contributed 30 ppm to the chemical shift of ¹³⁹La, while each ligand nitrogen atom contributed 50 ppm. This same empirical relationship does not hold for yttrium(III) complexes because the range of NMR chemical shifts observed for the two trivalent ions is quite different. Nevertheless,

if one makes the same assumption that each ligand nitrogen atom contributes equally and each oxygen atom contributes equally to the ^{89}Y chemical shift, the ^{89}Y chemical shifts of some of the yttrium(III) complexes listed in Table 2 are rather poorly predicted. An inspection of the ^{89}Y chemical shift data reported in Table 2 shows that generally ten-coordinated complexes (that is, $[\text{Y}(\text{BP18C6})]^+$ and $[\text{Y}(\text{P2C14Et4})]^{3+}$) give signals at higher fields, while the ^{89}Y resonances of eight-coordinate complexes are more deshielded and nine-coordinated complexes give signals in an intermediate range. Furthermore, the replacement of inner-sphere water molecules in $[\text{Y}(\text{EDTA})(\text{H}_2\text{O})_2]^-$ for ligands with different oxygen donor atoms as lactate affects drastically the value of the ^{89}Y NMR chemical shift (Supporting Information, Figure S8). This supports the use of different shielding constants for ligands having oxygen donor atoms of water, hydroxy, or carboxylate groups. In the other hand, the ^{89}Y NMR chemical shifts measured for thermally polarized samples of complexes $[\text{Y}(\text{DOTAM-2C})]^-$, $[\text{Y}(\text{DOTAM-3C})]^-$, and $[\text{Y}(\text{DOTAM-5C})]^-$ are very similar to that of $[\text{Y}(\text{DOTA}(\text{gly})_4)]^-$ (Table 2; Figure S9, Supporting Information). The varying lengths of the four side chains of the ligand have an effect on the inversion of the population of the twisted-square antiprismatic (TSAP) and square antiprismatic (SAP) diastereomers. Therefore, it turns out that chemical shifts are mainly dependent of contribution from the coordinated atoms rather than other structural factors. Thus, we attempted to fit the experimental ^{89}Y NMR data to an empirical relationship of the form:

$$\delta^{\text{calc}}(^{89}\text{Y}) = A - (S_{\text{Nam}} \cdot n_{\text{Nam}} + S_{\text{Npy}} \cdot n_{\text{Npy}} + S_{\text{Oc}} \cdot n_{\text{Oc}} + S_{\text{Oh}} \cdot n_{\text{Oh}} + S_{\text{Oe}} \cdot n_{\text{Oe}} + S_{\text{Oa}} \cdot n_{\text{Oa}} + S_{\text{Ow}} \cdot n_{\text{Ow}}) \quad (3)$$

where A is an empirical constant that can be regarded as the chemical shift of Y^{3+} in the absence of any ligand, S_{Nam} , S_{Npy} , S_{Oc} , S_{Oh} , S_{Oe} , S_{Oa} , and S_{Ow} represent the shielding contribution of amine, pyridine, carboxylate, hydroxy, ether, amide, and water donor atoms and n_{Nam} , n_{Npy} , n_{Oc} , n_{Oh} , n_{Oe} , n_{Oa} , and n_{Ow} are the number of donor atoms of each class. The use of different shielding constants for similar donor atoms such as amide or carboxylate oxygen atoms is justified by the different chemical shifts observed for $[\text{Y}(\text{DOTA})(\text{H}_2\text{O})]^-$ (111 ppm) and $[\text{Y}(\text{DOTAM})(\text{H}_2\text{O})]^{3+}$ (123 ppm),^[45] which indicate that oxygen atoms of carboxylate groups provide a slightly more important contribution to the shielding of the ^{89}Y NMR resonance than amide oxygen atoms. The best fit of the data provided $A=863\pm 48$ ppm and the shielding constants reported in Table 2.

The shielding effect of an amine nitrogen atom ($S_{\text{Nam}}=68.1$ ppm) is considerably smaller than that of pyridyl nitrogen atoms ($S_{\text{Npy}}=85.7$ ppm). Oxygen donor atoms of organic ligands provoke rather similar shielding effects (94.0–97.3 ppm), while the shielding contribution of water molecules is significantly higher ($S_{\text{Ow}}=107.6$ ppm). Figure 6 shows a plot of experimental versus calculated ^{89}Y NMR shifts obtained with Equation (3) for 21 complexes. The shifts of NTA^{3-} and NTPA^{3-} complexes were found to deviate considerably from the predicted values, and were omitted from Figure 6. The reasons for this discrepancy are likely related to the presence of hydration equilibria in solution, as discussed below. Nevertheless, the error between the calculated versus experimental data for the 21 complexes is relatively small (± 6.9 ppm).

Given the good agreement between the observed and calculated ^{89}Y NMR shifts for most systems, the noticeable deviations from the experimental and calculated data of $[\text{Y}(\text{NTA})_2]^{3-}$ and $[\text{Y}(\text{NTPA})_2]^{3-}$ are intriguing. In the case of $[\text{Y}(\text{NTA})_2]^{3-}$, Equation (3) predicts a shift of 55.2 ppm assuming the presence of a coordinated water molecule and 162.8 ppm if the complex lacks inner-sphere water molecules. The experimental shift (73.0 ppm) is closer to the value calculated for the $q=0$ species. In the case of $[\text{Y}(\text{NTPA})_2]^{3-}$ the donor atoms of the ligands are identical to those of $[\text{Y}(\text{NTA})_2]^{3-}$, leading to the same

calculated values. However, the experimental value is quite different (90.5 ppm). We interpret these data in terms of hydration equilibria involving a non-hydrated species and a complex species containing one coordinated water molecule. The calculated ^{89}Y NMR shifts suggest that the major species in solution corresponds to the hydrated complex, the population of the $q=0$ species being estimated as circa 15 and 30 % for $[\text{Y}(\text{NTA})_2]^{3-}$ and $[\text{Y}(\text{NTPA})_2]^{3-}$, respectively. Similar hydration equilibria involving complex species containing four- and five-coordinated water molecules are probably present in solutions of the $[\text{Y}(\text{NTA})]$ and $[\text{Y}(\text{NTPA})]$ complexes (Table 2).

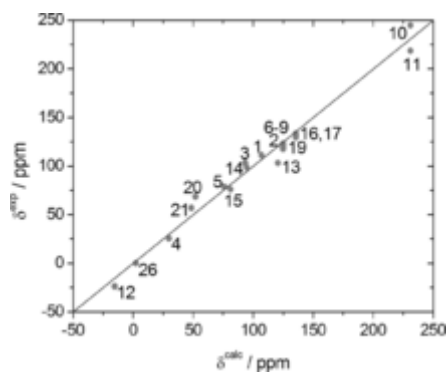


Figure 6. Plot of experimental ^{89}Y chemical shifts versus those predicted by Equation (3). The straight line is the identity line.

The $[\text{Y}(\text{TTHA})]^{3-}$ complex presents at least two species in solution at about neutral pH, as two signals at 103.2 ppm and 96.9 ppm are observed in the hyperpolarized ^{89}Y NMR spectrum at pH 6.9 (Table 1). The Ln^{3+} complexes of TTHA^{6-} form different structures in the solid state depending upon the size of the metal ion.^[46] The smallest Ln^{3+} ions form nine-coordinated complexes through binding of four amine nitrogen atoms and five oxygen atoms of carboxylate groups, the remaining carboxylate unit remaining uncoordinated. For the largest Ln^{3+} ions, ten-coordinate species were observed in the solid state thanks to the coordination of the four amine nitrogen atoms and the six carboxylate oxygen atoms. Additionally, dinuclear $[\text{Ln}_2(\text{HTTHA})_2]^{4-}$ species containing nine-coordinated metal ions were also reported, with the metal coordination environment being fulfilled by three amine nitrogen atoms, four carboxylate groups of one of the ligands, and two carboxylate groups of a neighboring ligand unit. The chemical shift values calculated with Equation (3) for the nine- and ten-coordinated $[\text{Y}(\text{TTHA})]^{3-}$ species are 120.6 ppm and 26.6 ppm, respectively. The calculated value for the dinuclear $[\text{Ln}_2(\text{HTTHA})_2]^{4-}$ species is 94.7 ppm. The latter value is in excellent agreement with the NMR signal observed at 96.9 ppm. Thus, most likely the Y^{3+} -TTHA complex is present in solution as a mixture of a mononuclear and a dinuclear species, giving ^{89}Y NMR signals at 103.2 and 96.9 ppm, respectively. A minor amount of ten-coordinate $[\text{Y}(\text{TTHA})]^{3-}$ species might be responsible for the 17.5 ppm difference between the experimental and calculated shifts of $[\text{Y}(\text{TTHA})]^{3-}$.

DFT calculations

Aiming to have a deeper insight on the origin of the ^{89}Y NMR chemical shifts observed for polyaminocarboxylate complexes, we turned our attention to theory. Prior to calculation of ^{89}Y NMR chemical shifts using DFT methods, we first performed geometry optimizations of 16 Y^{3+} complexes with polyaminocarboxylates using the TPSSh functional and a quasirelativistic pseudopotential that includes the inner 28 electrons in the core (see computational details below). For those complexes containing coordinated water molecules, we explicitly included two second-sphere water molecules hydrogen-bonded to each coordinated water molecule, as the inclusion of second-sphere water molecules was found to be critical for an accurate calculation of Gd^{3+} - O_{water} distances and ^{17}O hyperfine coupling constants in Gd^{3+} complexes of

polyaminocarboxylates.^[47, 48] The optimized geometries of all Y^{3+} complexes together with the calculated bond distances of the Y^{3+} coordination environments are shown in the Supporting Information, Figures S10, S11). The quality of the optimized structures was assessed by comparison of the calculated bond distances of the metal coordination environment with crystallographic data (Supporting Information, Tables S1–S3).

Since Y^{3+} is a relatively heavy atom, relativistic effects are expected to play an important role on the ^{89}Y NMR shifts.^[49] Thus, the absolute shielding constants were obtained using relativistic DFT calculations at the TPSSh/DKH2/TZVP level. A plot of the isotropic nuclear shielding values (σ_{iso}) versus the observed ^{89}Y NMR shifts provides a rather good linear correlation (Figure 7). Furthermore, the chemical shifts obtained using the σ_{iso} value calculated for $[Y(H_2O)_8]^{3+}$ are also in reasonable agreement with the experimental values (Table 3). Besides, these calculations allowed us to assess the hydration number of those complexes for which the number of coordinated water molecules was uncertain. One of such cases is $[Y(DO3A)(H_2O)_q]$, for which the ^{89}Y NMR shift calculated for the bis-hydrated complex (103.4 ppm, Table 3) is virtually identical to the experimental one (103.5 ppm). In contrast, the mono-hydrated complex yields a calculated chemical shift of 181.8 ppm, a value that deviates by about 78 ppm from the experimental one. For $[Y(EDTA)(H_2O)_q]^-$, the DFT calculations predict ^{89}Y NMR shifts of 20.5 and 119.4 ppm for the tris- and bis-hydrated forms, the latter value being in reasonably good agreement with the experimental one (135.7 ppm). However, for $[Y(NTA)_2(H_2O)_q]^{3-}$ the chemical shifts calculated for both the $q=1$ (24.3 ppm) and $q=0$ (101.8 ppm) species deviate considerably from the experimental value (73.0 ppm), suggesting that a hydration equilibrium exists in solution involving a mono- and a bis-hydrated species. The presence of hydration equilibria in solution was ascertained using absorption spectroscopy for different Eu^{3+} complexes, and therefore it is likely that some Y^{3+} complexes will show similar behavior.^[50, 51]

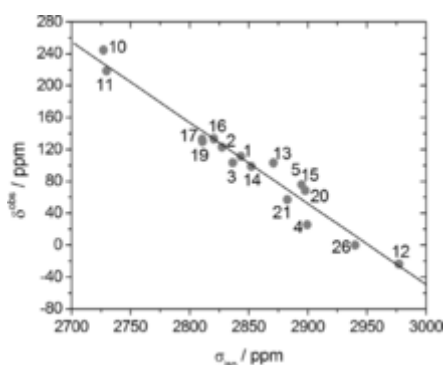


Figure 7. Plot of the experimental ^{89}Y NMR shifts versus the isotropic nuclear shielding values calculated in aqueous solution (COSMO) at the TPSSh/DKH2/TZVP level.

The calculated σ_{iso} values provide a rather good linear correlation with the calculated electron density at the Y^{3+} nucleus (Supporting Information, Figure S12). The σ_{iso} values can be broken down into the diamagnetic (σ^d) and paramagnetic (σ^p) contributions, which were obtained using each nucleus as the *gauche* origin for separation (Table 3).^[52] The diamagnetic contribution arises from the magnetic field at the nucleus produced by the diamagnetic current density caused in the electrons by the external magnetic field.^[53] Excluding the aquated ion, for the series of complexes listed in Table 3 the diamagnetic contribution varies by up to about 169 ppm. The σ^d values calculated for the complexes with polyaminocarboxylate ligands are larger than that calculated for $[Y(H_2O)_8]^{3+}$, which shows that the diamagnetic contribution provides a shielding effect to the ^{89}Y NMR shifts. The analysis of the natural electron configurations obtained for Y^{3+} in this series of complexes with Natural Bond Orbital (NBO) analysis provides some insight into the nature of this shielding

effect (Supporting Information, Table S4). The natural electron configurations reveal significant changes in the 5s and 4d populations depending upon the metal coordination environment. The 5s populations are relatively small and vary from 0.162 for [Y(EDTA)(H₂O)₂]⁻ to 0.186 for [Y(IMDA)₃]³⁻, while the calculated 4d populations present values in the range 0.82–1.08. The 5p populations are smaller (<0.014) than the 5s and 4d populations, as would be expected. Plots of the diamagnetic shielding contribution versus the calculated 4d, 5s, and 5p populations (Supporting Information, Figure S13) reveal linear trends that indicate increasing shielding effects upon increasing the population of the Y³⁺ valence orbitals.

Table 3. Isotropic ⁸⁹Y nuclear shielding values (σ_{iso}), diamagnetic (σ^{d}) and paramagnetic (σ^{p}) contributions to σ_{iso} , and ⁸⁹Y NMR shifts calculated in aqueous solution (COSMO) at the TPSSh/DKH2/TZVP level.

Y ³⁺ complex	σ_{iso}	σ^{d}	σ^{p}	δ^{calc}
[Y(DOTA)(H ₂ O)] ⁻ (1)	2843.6	4469.5	-1625.8	96.4
[Y(DOTAM)(H ₂ O)] ³⁺ (2)	2827.6	4464.8	-1637.6	112.4
[Y(DO3 A)(H ₂ O) ₂] (3)	2836.6	4464.9	-1628.3	103.4
[Y(P2C14Et4)] ³⁺ (4)	2899.6	4521.6	-1622.0	40.4
[Y(Me2DO2PA)] ⁺ (10)	2727.2	4461.4	-1734.2	212.8
[Y(CB-TE2PA)] ⁺ (11)	2729.9	4494.0	-1764.2	210.1
[Y(BP18C6)] ⁺ (12)	2977.3	4547.7	-1570.4	-37.3
[Y(TTHA)] ³⁻ (13)	2871.1	4489.1	-1618.0	68.9
[Y(IMDA) ₃] ³⁻ (14)	2852.3	4378.4	-1526.1	87.7
[Y(DTPA)(H ₂ O)] ²⁻ (15)	2894.9	4446.1	-1551.2	45.1
[Y(EDTA)(H ₂ O) ₂] ⁻ (16)	2820.6	4386.6	-1565.9	119.4
[Y(DCTA)(H ₂ O) ₂] ⁻ (17)	2810.8	4440.9	-16 300	129.2
[Y(DPTA)(H ₂ O) ₂] ⁻ (19)	2810.9	4407.4	-1596.5	129.1
[Y(EGTA)(H ₂ O)] ⁻ (20)	2898.0	4437.5	-1539.5	42.0
[Y(HIDA) ₂] ⁻ (21)	2882.8	4406.6	-1523.8	57.2
[Y(H ₂ O) ₈] ³⁺ (26)	2940.0	4060.5	-1120.6	0.0

The paramagnetic contribution accounts for the mixing of certain excited states with the electronic ground state in the presence of a magnetic field. The calculated σ^p values for complexes with polyaminocarboxylate ligands are more negative than that obtained for $[\text{Y}(\text{H}_2\text{O})_8]^{3+}$, indicating that the paramagnetic contribution results in a deshielding effect in the family of Y^{3+} complexes investigated here. The σ^p term generally becomes more important as the HOMO–LUMO gap is reduced (Supporting Information, Figure S14). This is expected as smaller HOMO–LUMO gaps tend to decrease the energy differences between all occupied and unoccupied orbitals.^[54]

Conclusion

This study has shown that Y^{3+} complexes with polyaminocarboxylate ligands provide a rather wide range of ^{89}Y NMR chemical shifts that spans about 270 ppm, an expansion by about 200 ppm of the chemical shift range observed previously. The ^{89}Y NMR chemical shifts can be obtained either using hyperpolarized samples or ^1H , ^{89}Y -HMQC NMR experiments to overcome the long acquisition times required for traditional ^{89}Y NMR experiments owing to the long relaxation times. The ^{89}Y NMR chemical shift values were found to change considerably depending upon the coordination number of the complex and the nature of the donor atoms of the ligand. A relativistic DFT study was conducted to rationalize the origin of the ^{89}Y NMR chemical shifts. These calculations can predict the observed chemical shifts to a rather good accuracy. The breakdown of the calculated isotropic shielding constants revealed that the calculated ^{89}Y NMR chemical shifts are a subtle balance of the two contributions. Generally increased 4d, 5s, and 5p populations and large HOMO–LUMO gaps have a shielding effect on the ^{89}Y chemical shifts. However, these general trends do not allow a prediction of the chemical shifts without performing the DFT calculations. Thus, we proposed an empirical relationship that provides calculated chemical shifts to an accuracy of about ± 6.9 ppm with respect to the experimental values. This empirical expression will be useful for the rational design of ^{89}Y NMR imaging probes for hyperpolarized imaging. Furthermore, the ^{89}Y NMR chemical shifts are also useful to gain information on the solution structure of the corresponding complexes with Ln^{3+} ions.

Experimental Section

General: All chemicals used were of the highest available purity and were not purified further. Solvents used were available commercially and used as received. Yttrium nitrate hexahydrate was obtained from Aldrich. Syntheses performed under microwave radiation were carried out with a Monowave Anton Paar 300 instrument (30 bar/850W). Elemental analyses were performed in a Carlo–Erba EA 1108 microanalyzer. Attenuated total reflection infrared (ATR-FTIR) spectra were recorded on a FP-6100 Jasco spectrometer. ESI-MS experiments of complexes $[\text{Y}(\text{P2C14Et4})(\text{NO}_3)_3 \cdot 6 \text{H}_2\text{O}]$ and $[\text{Y}(\text{P2C14Py4})(\text{NO}_3)_3 \cdot 6 \text{H}_2\text{O}]$ were performed on a microTOF(focus) mass spectrometer (Bruker Daltonics, Bremen, Germany). Ions were generated using an ApolloII (ESI) source and ionization was achieved by electrospray. ESI-MS analyses of the remaining complexes were done either at HT Laboratory (San Diego, CA) or at core facilities at UT Southwestern Medical Center at Dallas. The pH values were direct readings as measured on an Orion 720 A+ (Thermo Corporation, city, state) or an Ultra Basic 5 pH meter (Denver Instruments, city state).

NMR spectroscopy: One-dimensional ^1H NMR spectra of compounds $[\text{Y}(\text{P2C14Et4})(\text{NO}_3)_3 \cdot 6 \text{H}_2\text{O}]$, $[\text{Y}(\text{P2C14Py4})(\text{NO}_3)_3 \cdot 6 \text{H}_2\text{O}]$, $[\text{Y}(\text{Me2DO2PA})\text{Cl}]$, and $[\text{Y}(\text{CB-TE2PA})\text{Cl}]$ were recorded at 25 °C on a BRUKER Avance III HD 500 spectrometer equipped with an indirect 5 mm triple resonance broad band (TBI) $^1\text{H}/\{\text{BB}\}/^{13}\text{C}$ probe. Spectra were performed according to BRUKER's pulse programs with standard pulse sequences using delay times of 2 s, a 30° pulse, and 16 scans. The ^{89}Y chemical shifts were obtained using heteronuclear multiple quantum coherence ^1H – ^{89}Y (HMQC) experiments with a delay for evolution of

long-range couplings of 41.66 ms and a 2 s delay for relaxation time. For example, in an HMQC experiment, the raw data set consisted of 48 fid of 1024 (F2) \times 98(F1) complex data points, each zero-filled to 1000 in the F1 dimension prior to Fourier transform with a spectral width of 31 846 Hz and 4504 Hz in the F1 and F2 dimensions, respectively. ^1H Chemical shifts were expressed in ppm relative to TSP as external reference, in 99.97 % D_2O , and TMS for others solvents. ^{89}Y chemical shifts were expressed in ppm relative to yttrium nitrate hexahydrate 1 m, pH 4.3 as external reference. The one-dimensional ^{89}Y spectrum reference was recorded with a 50 s delay relaxation time, 976 scans, and a spectral window of 5980 Hz. ^1H , ^{13}C , and thermally polarized ^{89}Y NMR spectra of all other complexes were recorded using a Bruker Avance III 400 MHz spectrometer and a 5 mm sample probe. Hyperpolarized ^{89}Y NMR spectra were collected at a field strength of 9.4 T at 25° on an Oxford unshielded 89 mm magnet with Varian 10 mm low gamma probe. Both hyperpolarized and thermally polarized ^{89}Y NMR spectra were referenced to YCl_3 at 0 ppm.

Hyperpolarization experiments: Hyperpolarization of $[\text{Y}(\text{EDTA})(\text{H}_2\text{O})_2]^-$ (0.158 m), $[\text{Y}(\text{EGTA})(\text{H}_2\text{O})]^-$ (0.200 m), $[\text{Y}(\text{TTHA})]^{3-}$ (0.200 m), $[\text{Y}(\text{NTA})_2]^{3-}$ (0.187 m), $[\text{Y}(\text{DTPA})(\text{H}_2\text{O})_2]^-$ (0.160 m), $[\text{Y}(\text{DOTA})(\text{H}_2\text{O})]^-$ (0.397 m), and $[\text{Y}(\text{DO3 A})(\text{H}_2\text{O})_2]$ (0.187 m) were generated following a reported method.^[7] After 4.16 mL of hyperpolarized $[\text{Y}(\text{EDTA})(\text{H}_2\text{O})_2]^-$ solution was ejected from the HyperSense, 1 mL was transferred to a 10 mm NMR tube to acquire the ^{89}Y NMR data. Hyperpolarized ^{89}Y spectra of $[\text{Y}(\text{TTHA})]^{3-}$ were collected at pH 4.8 and 6.9 in buffer solutions.

Crystal structure determinations: X-ray diffraction data for compound $[\text{Y}(\text{P2C14Et4})](\text{NO}_3)_3 \cdot 6 \text{H}_2\text{O}$ were collected at 173 K on a Bruker Smart-CCD- 6000 using Cu-K α radiation. All data were corrected by Lorentz and polarization effects. Empirical absorption corrections were also applied.^[55] Complex scattering factors were taken from the program package SHELX-97.^[56] The structure was solved by direct methods using SIR-92,^[57] which revealed the position of all non-hydrogen atoms. The structure was refined on F^2 by a full-matrix least-squares procedure using anisotropic displacement parameters for all non-hydrogen atoms. The hydrogen atoms bonded to carbon atoms were located in their calculated positions and refined using a riding model. For compounds $[\text{Y}(\text{Me2DO2PA})](\text{PF}_6) \cdot 2\text{H}_2\text{O}$ and $[\text{Y}(\text{CB-TE2PA})](\text{PF}_6) \cdot 2.5\text{H}_2\text{O}$ single-crystal X-ray diffraction data were collected with a Xcalibur 2 CCD 4-circle Diffractometer (Oxford Diffraction) fitted with a graphite monochromated MoK α radiation ($\lambda=0.71073 \text{ \AA}$). Data were collected at 170 K and 298 K. Unit cell determination and data reduction, including interframe scaling, Lorentzian, polarization, empirical absorption, and detector sensitivity corrections, were carried out using attached programs of CrysAlis software (Oxford Diffraction).^[58] Structures were solved by direct methods and refined by full matrix least-squares method on F^2 with the SHELX L97^[56] suite of programs. The hydrogen atoms were identified at the last step and refined under geometrical restraints and isotropic U-constraints.

Crystal data and structure refinement details are given in the Supporting Information, Table S5. CCDC 1484094, 1484140, and 1484139 contain the supplementary crystallographic data for this paper. These data are provided free of charge by The Cambridge Crystallographic Data Centre. Molecular graphics were generated by using USCF Chimera (version 1.8).^[59]

Preparation of the complexes: Yttrium complexes derived from ligands EDTA, EGTA, TTHA, DTPA, DO3A, NTA, DOTA, DOTA-(gly)₄, DOTAM-2C, DOTAM-3C, DOTAM-5C, were synthesized following reported procedures.^[7, 60] MS (ESI⁻, H_2O): m/z 377.00 (100 %) $[\text{Y}(\text{EDTA})]^-$; 465.07 (100 %) $[\text{Y}(\text{EGTA}-4\text{H})]^-$; 579.20 (30 %) $[\text{Y}(\text{H}_2\text{TTHA})]^-$; 601.13 (100 %) $[\text{Y}(\text{HTTHA})+\text{Na}]^-$; 467.00 (52 %) $[\text{Y}(\text{NTA})_2-4\text{H}]^-$; 511.07 (88 %) $[\text{Y}(\text{NTA})_2+2\text{Na}]^-$; 489.00 (100 %) $[\text{Y}(\text{NTA})(\text{HNTA})+\text{Na}]^-$; 489.5 (100 %) $[\text{Y}(\text{DOTA})]^-$; 238.4 (100 %) $[\text{Y}(\text{DTPA})]^{2-}/2$; 773.53 (100 %) $[\text{Y}(\text{DOTAM-2C})]^-$; 829.60 (100 %) $[\text{Y}(\text{DOTAM-3C})]^-$; 941.73 (100 %) $[\text{Y}(\text{DOTAM-5C})]^-$. MS (ESI⁺): m/z 741.87 (100 %) $[\text{Y}(\text{HDOTA}-(\text{Gly})_4)+\text{Na}]^+$; 455.20 (100 %) $[\text{Y}(\text{DO3 A})+\text{Na}]^+$; 571.20 (80 %) $[\text{Y}(\text{DO3A})+3\text{Na}+2\text{Cl}]^+$.

General procedure for the syntheses of $[\text{Y}(\text{P2C14Et4})](\text{NO}_3)_3 \cdot 6 \text{H}_2\text{O}$ and $[\text{Y}(\text{P2C14Py4})](\text{NO}_3)_3 \cdot 6 \text{H}_2\text{O}$: A solution of $\text{Y}(\text{NO}_3)_3 \cdot 6 \text{H}_2\text{O}$ (0.04 mmol) in methanol (5 mL) was added to a stirred solution of the

appropriate ligand (0.04 mmol) in the same solvent (10 mL). The solution was allowed to concentrate and the crude products were recrystallized in water. By slow concentration of the water solutions, crystalline products were obtained, which were filtered off and air-dried.

[Y(P2C14Et4)](NO₃)₃·6 H₂O: Yield: 67 %; ¹H NMR (500 MHz, D₂O, pD=7.46, 25 °C): δ=8.00 (t, ³J=7.8 Hz, 2 H, py), 7.51 (d, ³J=7.8 Hz, 4 H, py), 4.68 (d, ²J=16.3 Hz, 4 H, CH_{2eq}-py), 4.17 (td, ²J=10.9 Hz, ³J=6.7 Hz, 4 H, CH_{2ax}-OH), 3.88 (m, 4 H, -CH_{2ax}-py), 3.86 (m, 4 H, -CH_{2eq}-OH), 3.59 (d, ³J=9.9 Hz, 4 H, CH_{2eq}(ethyl)), 3.26-3.19 (m, 4 H, CH_{2ax}-N), 2.68 (td, ²J=10.9 Hz, ³J=6.7 Hz, 4 H, CH_{2eq}-N), 2.57 ppm (d, ³J=9.9 Hz, 4 H, CH_{2ax} (ethyl)); IR (ATR): ν=1607 (s), 1457 (s) (C=C) and (C=N)_{py}, 2868 (m), 2763 (m) (OH), 1329 (s), 827 (m), 736 (m) (NO₃⁻); MS (ESI⁺): *m/z* 589.22 (100 %) [Y(P2C14Et4)-2H]⁺, 737.19 (4 %) [Y(P2C14Et4)+Na+2(NO₃)-H]⁺; elemental analysis calcd (%) for C₂₆H₅₄N₉O₁₉Y: C 35.3, H 6.2, N 14.2; found: C 35.1, H 6.4, N 14.3.

[Y(P2C14Py4)](NO₃)₃·6 H₂O: Yield: 66 %; ¹H NMR (500 MHz, D₂O, pD=7.46, 25 °C): δ=8.46 (t, ³J=7.9 Hz, 2 H, py), 7.97 (d, ³J=7.9 Hz, 4 H, py), 7.56 (t, ³J=7.7 Hz, 4 H, -(py)₄), 7.27 (d, ³J=7.7 Hz, 4 H, (py)₄), 7.07 (t, ³J=6.6 Hz, 4 H, (py)₄), 6.87 (m, 4 H, (py)₄), 4.74 (d, ³J=16.6 Hz, 4 H, (CH_{2eq}-py)₄), 4.59 (d, ³J=17.5 Hz, 4 H, CH_{2eq}-py), 4.03 (d, ³J=16.6 Hz, 4 H, (CH_{2ax}-py)₄), 3.78 (d, ³J=17.5 Hz, 4 H, CH_{2ax}-py), 3.18 (d, ³J=10.0 Hz, 4 H, CH_{2eq}-(ethyl)), 2.43 ppm (d, ³J=10.0 Hz, 4 H, CH_{2ax}-(ethyl)); IR (ATR): ν=1602 (s), 1457 (s) (C=C) and (C=N)_{py}, 1324 (s), 817 (m), 828 (m), 760 (m) (NO₃⁻); MS (ESI⁺): *m/z* 903.3 (70 %) [Y(P2C14Py4)(NO₃)₂]⁺, 420.6 (100 %) [Y(P2C14Py4)(NO₃)₃]²⁺; elemental analysis calcd (%) for C₄₂H₅₈N₁₃O₁₅Y: C 47.0, H 5.4, N 17.0; found: C 47.0, H 5.7, N 16.8.

[Y(Me2DO2PA)]Cl: This complex was synthesized following a reported procedure.^[18] To a solution of Me2DO2PA·4 HCl (50 mg, 0.081 mmol) and Et₃N (66 mg, 0.649 mmol) in MeOH (4 mL) was added a solution of YCl₃·6 H₂O (37 mg, 0.122 mmol) in MeOH (3 mL). The mixture was heated to reflux during 72 h and then concentrated to dryness. The residue was stirred in CH₃CN (2 mL) at room temperature during 24 h. The precipitate was filtered and rinsed with CH₃CN (2 mL) and Et₂O (2 mL) to yield 34 mg of a white solid. Addition of an excess of KPF₆ to a solution of the complex gave single crystals suitable for X-ray diffraction analysis. Yield 71 %; ¹H NMR (500 MHz, D₂O, pD=7.46, 25 °C): δ=8.31 (m, 2 H, py), 8.07 (d, ³J=7.5 Hz, 2 H, py), 7.91 (d, ³J=9.0 Hz, 2 H), 4.86 (d, ²J=16.5 Hz, 2 H, -CH₂py), 4.29 (d, ²J=16.5 Hz, 2 H, CH₂py), 3.69 (s *br*, 4 H, CH₂ cyclen), 3.4–2.7 (m, 10 H, CH₂ cyclen), 2.33 (d, ²J=14.5 Hz, 2 H, CH₂cyclen), 2.10 ppm (s, 6 H, CH₃). ¹³C NMR (125.77 MHz, D₂O, pD=7.46, 25 °C): δ=174.22, 158.99, 152.13 (quaternary C); 145.74, 129.87, 127.06 (tertiary C); 58.47, 56.17 (secondary C); 47.76 ppm (primary C).

[Y(CB-TE2 PA)]Cl: This complex was prepared following the previously reported procedure.^[21] A mixture containing H₂CB-TE2PA·4 HCl (50 mg, 0.078 mmol), DIPEA (80 mg, 0.624 mmol), and YCl₃·6 H₂O (47 mg, 0.156 mmol) in *n*-butanol (10 mL) was heated at 150 °C during 4 h under microwave radiation. The solvent was evaporated and the solid was washed four times with THF. The complex was obtained as a brown solid (28 mg). Addition of an excess of KPF₆ to a solution of the complex gave single crystals suitable for X-ray diffraction analysis. Yield: 58 %; ¹H NMR (500 MHz, D₂O, pD=5.65, 25 °C): δ=8.21 (t, ³J=7.9 Hz, 2 H, py), 7.96 (d, ³J=7.9 Hz, 2 H, py), 7.82 (d, ³J=7.9 Hz, 2 H, py), 5.11 (d, ²J=15.3 Hz, 2 H, CH_{2ax}-py), 4.15 (d, ²J=15.3 Hz, 2 H, CH_{2eq}-py), 3.7–3.6 (m, 4 H), 3.10–3.01 (m, 2 H), 2.96–2.80 (m, 6 H), 2.72–2.69 (m, 2 H), 2.50–2.41 (m, 2 H), 2.4–2.25 (m, 4 H), 2.0–1.9 (m, 2 H), 1.3 ppm (m, 2 H). ¹³C NMR (75.47 MHz, D₂O, pD=5.65, 25 °C): δ=175.80, 159.56, 151.96 (quaternary C); 145.62, 129.08, 126.00 (tertiary C); 71.52, 62.22, 62.10, 60.74, 55.91, 55.62, 26.88 ppm (secondary C).

Computational details: Geometry optimizations were performed in aqueous solution employing DFT within the hybrid meta-GGA approximation with the TPSSh exchange-correlation functional,^[61] and the Gaussian 09 package (Revision D.01).^[62] In these calculations we used the quasi-relativistic effective core potential ECP28 MWB of Preuss et al.^[63] and the related (8s7p6d2f1g)/[6s5p3d2f1g]-GTO valence basis set for Y,^[63, 64] in combination with the standard 6-31G(d,p) basis set for the ligand atoms. No symmetry

constraints have been imposed during the optimizations. The default values for the integration grid (75 radial shells and 302 angular points) and the SCF energy convergence criteria (10^{-8}) were used in all calculations. The stationary points found on the potential energy surfaces as a result of the geometry optimizations have been tested to represent energy minima rather than saddle points via frequency analysis. Bulk solvent effects (water) were included with the polarizable continuum model using the integral equation formalism (IEFPCM)^[65] variant as implemented in Gaussian 09. The universal force field radii (UFF)^[66] scaled by a factor of 1.1 were used to define the solute cavities.

The calculations of the ⁸⁹Y NMR shielding tensors were carried out using the ORCA program package (Version 3.0.1)^[67] using the own nucleus as the origin of this gauche origin. Relativistic effects were considered by means of the second order Douglas–Kroll–Hess (DKH2) method,^[68] with the all-electron scalar relativistic TZVP-DKH basis set of Pantazis et al. for Y.^[69] The geometries of the complexes optimized with the Gaussian code as described above were employed. The RIJCOSX approximation^[70] was used to speed up the calculations of NMR parameters using the Def2-TZVPP/JK^[71] auxiliary basis set as constructed automatically by ORCA. The convergence tolerances and integration accuracies of the calculations were increased from the defaults using the available TightSCF and Grid5 options. Solvent effects (water) were taken into account by using the COSMO solvation model as implemented in ORCA.^[72] Chemical shifts were calculated as $\delta = (\sigma^{\text{ref}} - \sigma)$ using $[\text{Y}(\text{H}_2\text{O})_8]^{3+}$ as a reference. Natural electron configurations were obtained with the NBO 6.0 program developed by Weinhold.^[73]

Acknowledgements

The authors are indebted to Centro de Supercomputación de Galicia (CESGA) for providing the computer facilities. M.R.-F., D.E.-G., and C.P.-I. thank Ministerio de Economía y Competitividad (CTQ2013-43243-P and CTQ2015-71211-REDT) for generous financial support. R.T. acknowledges the Ministère de l'Enseignement Supérieur et de la Recherche, the Centre National de la Recherche Scientifique, and the “Service Commun” of NMR facilities of the University of Brest. C.P.-I. acknowledges the University of Brest for his invited Professor position. A.D.S. acknowledges financial support from the National Institutes of Health (EB-015908 and CA-115531) and the Robert A. Welch Foundation (AT-584).

[1] a) L. M. De Leon-Rodriguez, A. J. M. Lubag, C. R. Malloy, G. V. Martinez, R. J. Gillies, A. D. Sherry, *Acc. Chem. Res.* 2009, 42, 948–957; b) E. Terreno, D. D. Castelli, A. Viale, S. Aime, *Chem. Rev.* 2010, 110, 3019–3042.

[2] a) S. Aime, D. D. Castelli, S. G. Crich, E. Gianolio, E. Terreno, *Acc. Chem. Res.* 2009, 42, 822–831; b) P. Caravan, *Chem. Soc. Rev.* 2006, 35, 512–523.

[3] K. Golman, L. E. Olsson, O. Axelsson, M. Mansson, M. Karlsson, J. S. Peterson, *Br. J. Radiol.* 2003, 76, S118.

[4] B. M. Goodson, *Annu. Rep. NMR Spectrosc.* 2005, 55, 299–323.

[5] J. H. Ardenkjaer-Larsen, S. Macholl, H. Johannesson, *Appl. Magn. Reson.* 2008, 34, 509–522.

[6] M. E. Merritt, C. Harrison, Z. Kovacs, P. Kshirsagar, C. R. Malloy, A. D. Sherry, *J. Am. Chem. Soc.* 2007, 129, 12942–12943.

[7] A. K. Jindal, M. E. Merritt, E. H. Suh, C. R. Malloy, A. D. Sherry, Z. Kovacs, *J. Am. Chem. Soc.* 2010, 132, 1784–1785.

- [8] L. Lumata, A. K. Jindal, M. E. Merritt, C. R. Malloy, A. D. Sherry, Z. Kovacs, *J. Am. Chem. Soc.* 2011, 133, 8673–8680.
- [9] L. Lumata, M. Merritt, C. Malloy, A. D. Sherry, Z. Kovacs, *Appl. Magn. Reson.* 2012, 43, 69–79.
- [10] R. C. Holz, W. D. Horrocks, *J. Magn. Reson.* 1990, 89, 627–631.
- [11] R. D. Shannon, *Acta Crystallogr. Sect. A* 1976, 32, 751–767.
- [12] *The Chemistry of Contrast Agents in Medical Magnetic Resonance Imaging*, A. E. Merbach, L. Helm, É. Tóth, Eds., 2nd ed., Wiley, New York, 2013.
- [13] P. Verwilt, S. Park, B. Yoon, J. S. Kim, *Chem. Soc. Rev.* 2015, 44, 1791–1806.
- [14] C. Popovici, I. Fernández, P. Oña-Burgos, L. Rocas, S. García-Granda, F. L. Ortiz, *Dalton Trans.* 2011, 40, 6691–6703.
- [15] E. Brun, J. Oeser, H. H. Staub, C. G. Telschow, *Phys. Rev.* 1954, 93, 172–173.
- [16] a) R. M. Adam, G. V. Fazakerley, D. G. Reid, *J. Magn. Reson.* 1979, 33, 655–657; b) G. C. Levy, P. L. Rinaldi, J. T. Bailey, *J. Magn. Reson.* 1980, 40, 167–173.
- [17] M. del C. Fernández-Fernández, R. Bastida, A. Macías, P. Pérez-Lourido, C. Platas-Iglesias, L. Valencia, *Inorg. Chem.* 2006, 45, 4484–4496.
- [18] A. Rodríguez-Rodríguez, D. Esteban-Gómez, A. de Blas, T. Rodríguez-Blas, M. Fekete, M. Botta, R. Tripier, C. Platas-Iglesias, *Inorg. Chem.* 2012, 51, 2509–2521.
- [19] A. Rodríguez-Rodríguez, D. Esteban-Gómez, A. de Blas, T. Rodríguez-Blas, M. Botta, R. Tripier, C. Platas-Iglesias, *Inorg. Chem.* 2012, 51, 13419–13429.
- [20] G. Castro, M. Regueiro-Figueroa, D. Esteban-Gómez, R. Bastida, A. Macías, P. Pérez-Lourido, C. Platas-Iglesias, L. Valencia, *Chem. Eur. J.* 2015, 21, 18662–18670.
- [21] A. Rodríguez-Rodríguez, D. Esteban-Gómez, R. Tripier, G. Tircso, Z. Garda, I. Toth, A. de Blas, T. Rodríguez-Blas, C. Platas-Iglesias, *J. Am. Chem. Soc.* 2014, 136, 17954–17957.
- [22] A. Rodríguez-Rodríguez, M. Regueiro-Figueroa, D. Esteban-Gómez, R. Tripier, G. Tircso, F. K. Kálmán, A. C. Bényei, I. Tóth, A. de Blas, T. Rodríguez-Blas, C. Platas-Iglesias, *Inorg. Chem.* 2016, 55, 2227–2239.
- [23] A. Roca-Sabio, M. Mato-Iglesias, D. Esteban-Gómez, É. Tóth, A. de Blas, C. Platas-Iglesias, T. Rodríguez-Blas, *J. Am. Chem. Soc.* 2009, 131, 3331–3341.
- [24] M. Regueiro-Figueroa, D. Esteban-Gómez, A. de Blas, T. Rodríguez-Blas, C. Platas-Iglesias, *Chem. Eur. J.* 2014, 20, 3974–3981.
- [25] G. Castro, M. Regueiro-Figueroa, D. Esteban-Gómez, P. Pérez-Lourido, C. Platas-Iglesias, L. Valencia, *Inorg. Chem.* 2016, 55, 3490–3497.
- [26] C. A. Chang, L. C. Francesconi, M. F. Malley, K. Kumar, J. Z. Gougoutas, M. F. Tweedle, *Inorg. Chem.* 1993, 32, 3501–3508.
- [27] D. Parker, K. Pulukkody, F. C. Smith, A. Batsanov, J. A. K. Howard, *J. Chem. Soc. Dalton Trans.* 1994, 689–693.

- [28] F. Benetollo, G. Bombieri, L. Calabi, S. Aime, M. Botta, *Inorg. Chem.* 2003, 42, 148–157.
- [29] S. Aime, M. Botta, G. Ermondi, *Inorg. Chem.* 1992, 31, 4291–4299.
- [30] S. Amin, D. A. Voss Jr., W. D. Horrocks Jr., C. H. Lake, M. R. Churchill, J. R. Morrow, *Inorg. Chem.* 1995, 34, 3294–3300.
- [31] S. Aime, A. Barge, F. Benetollo, G. Bombieri, M. Botta, F. Uggeri, *Inorg. Chem.* 1997, 36, 4287–4289.
- [32] S. Aime, M. Botta, M. Fasano, M. P. M. Marques, C. F. G. C. Geraldès, D. Pubanz, A. E. Merbach, *Inorg. Chem.* 1997, 36, 2059–2068.
- [33] F. A. Dunand, R. S. Dichins, D. Parker, A. E. Merbach, *Chem. Eur. J.* 2001, 7, 5160–5167.
- [34] É. Tóth, O. M. N. Dhuhghaill, G. Nesson, L. Helm, A. E. Merbach, *Magn. Reson. Chem.* 1999, 37, 701–708.
- [35] X. Zhang, C. A. Chang, H. G. Brittain, J. M. Garrison, J. Telsler, M. F. Tweedle, *Inorg. Chem.* 1992, 31, 5597–5600.
- [36] S. Aime, A. Barge, A. Borel, M. Botta, S. Chemerisov, A. E. Merbach, U. Müller, D. Pubanz, *Inorg. Chem.* 1997, 36, 5104–5112.
- [37] L. Q. Zhang, T. T. Fan, J. Wang, B. Liu, D. Li, G. X. Han, R. Xu, X. D. Zhang, *Russ. J. Coord. Chem.* 2010, 36, 389–395.
- [38] J. A. Peters, *Inorg. Chem.* 1988, 27, 48486–44691.
- [39] J. Wang, D.-M. Fan, X.-D. Zhang, R. Ma, *Acta Chim. Sin.* 2002, 60, 536–540.
- [40] J. Wang, Y. Wang, Zh. H. Zhang, X. D. Zhang, J. Tong, X. Zh. Liu, X. Y. Liu, Y. Zhang, Zh. J. Pan, *J. Struct. Chem.* 2005, 46, 895–905.
- [41] S.-G. Lee, *Bull. Korean Chem. Soc.* 1996, 17, 589–591.
- [42] M. W. Löble, M. Casimiro, D. T. Thielemann, P. Oña-Burgos, I. Fernández, P. W. Roesky, F. Breher, *Chem. Eur. J.* 2012, 18, 5325–5334.
- [43] R. E. White, T. P. Hanusa, *Organometallics* 2006, 25, 5621–5630.
- [44] C. F. G. C. Geraldès, A. D. Sherry, *J. Magn. Reson.* 1986, 66, 274–282.
- [45] P. Mieville, S. Jannin, L. Helm, G. Bodenhausen, *J. Am. Chem. Soc.* 2010, 132, 5006–5007.
- [46] P. Caravan, J. J. Ellison, J. McMurry, B. Lauffer, *Chem. Rev.* 1999, 99, 2293–2352.
- [47] M. Regueiro-Figueroa, C. Platas-Iglesias, *J. Phys. Chem. A* 2015, 119, 6436–6445.
- [48] D. Esteban-Gómez, A. de Blas, T. Rodríguez-Blas, L. Helm, C. Platas-Iglesias, *ChemPhysChem* 2012, 13, 3640–3650.
- [49] J. Autschbach, *Philos. Trans. R. Soc. London Ser. A* 2014, 372, 20120489.
- [50] N. Graepi, D. H. Powell, G. Laurenczy, L. Zekany, A. E. Merbach, *Inorg. Chim. Acta* 1995, 235, 311–326.

- [51] a) C. Platas-Iglesias, D. M. Corsi, L. Vander Elst, R. N. Muller, D. Imbert, J.-C. G. Benzli, E. Toth, T. Maschmeyer, J. A. Peters, *Dalton Trans.* 2003, 727–737; b) E. Balogh, M. Mato-Iglesias, C. Platas-Iglesias, E. Toth, K. Djanashvili, J. A. Peters, A. de Blas, T. Rodriguez-Blas, *Inorg. Chem.* 2006, 45, 8719–8728.
- [52] a) J. A. Platts, K. Gkionis, *Phys. Chem. Chem. Phys.* 2009, 11, 10331–10339; b) A. H. Greif, P. Hrobarik, V. Hrobarikova, A. V. Arbuznikov, J. Autschbach, M. Kaupp, *Inorg. Chem.* 2015, 54, 7199–7208.
- [53] J. C. Facelli, *Prog. Nucl. Magn. Reson. Spectrosc.* 2011, 58, 176–201.
- [54] S. Moncho, J. Autschbach, *Magn. Reson. Chem.* 2010, 48, S76–S85.
- [55] G. M. Sheldrick, SADABS. Program for Empirical Absorption Correction of Area Detector Data. University of Göttingen, Germany, 1996.
- [56] G. M. Sheldrick, SHELX-97, An integrated system for solving and refining crystal structures from diffraction data, University of Göttingen, Germany 1997.
- [57] A. Altomare, G. Cascarano, C. Giacovazzo, A. Gualardi, *J. Appl. Crystallogr.* 1993, 26, 343–350.
- [58] CrysAlis software system, version 1.171.28 cycle 4 beta, Oxford Diffraction Ltd, Abingdon, U. K., 2005.
- [59] E. F. Pettersen, T. D. Goddard, C. C. Huang, G. S. Couch, D. M. Greenblatt, E. C. Meng, T. E. Ferrin, *J. Comput. Chem.* 2004, 25, 1605–1612.
- [60] M. P. Lowe, D. Parker, O. Reany, S. Aime, M. Botta, G. Castellano, E. Gianolio, R. Pagliari, *J. Am. Chem. Soc.* 2001, 123, 7601–7609.
- [61] J. M. Tao, J. P. Perdew, V. N. Staroverov, G. E. Scuseria, *Phys. Rev. Lett.* 2003, 91, 146401.
- [62] M. J. Frisch, G. W. Trucks, H. B. Schlegel, G. E. Scuseria, M. A. Robb, J. R. Cheeseman, G. Scalmani, V. Barone, B. Mennucci, G. A. Petersson, et al. Gaussian 09, Revision D.01, Gaussian, Inc.: Wallingford CT, 2009.
- [63] D. Andrae, U. Haeussermann, M. Dolg, H. Stoll, H. Preuss, *Theor. Chim. Acta* 1990, 77, 123–141.
- [64] J. M. L. Martin, A. Sundermann, *J. Chem. Phys.* 2001, 114, 3408–3420.
- [65] J. Tomasi, B. Mennucci, R. Cammi, *Chem. Rev.* 2005, 105, 2999–3093.
- [66] A. K. Rappe, C. J. Casewit, K. S. Colwell, W. A. Goddard III, W. M. Skiff, *J. Am. Chem. Soc.* 1992, 114, 10024–10035.
- [67] F. Neese, The ORCA program system, *WIREs Comput. Mol. Sci.* 2012, 2, 73–78.
- [68] a) M. Barysz, A. J. Sadlej, *J. Mol. Struct.* 2001, 573, 181–200; b) M. Reiher, *Theor. Chem. Acc.* 2006, 116, 241–252.
- [69] D. A. Pantazis, X. Y. Chen, C. R. Landis, F. Neese, *J. Chem. Theory Comput.* 2008, 4, 908–919.
- [70] a) F. Neese, F. Wennmohs, A. Hansen, U. Becker, *Chem. Phys.* 2009, 356, 98–109; b) R. Izsák, F. Neese, *J. Chem. Phys.* 2011, 135, 144105; c) T. Petrenko, S. Kossmann, F. Neese, *J. Chem. Phys.* 2011, 134, 054116; d) S. Kossmann, F. Neese, *Chem. Phys. Lett.* 2009, 481, 240–243.
- [71] F. Weigend, R. Ahlrichs, *Phys. Chem. Chem. Phys.* 2005, 7, 3297–3305.

- [72] S. Sinnecker, A. Rajendran, A. Klamt, M. Diedenhofen, F. Neese, *J. Phys. Chem. A* 2006, 110, 2235–2245.
- [73] NBO 6.0. E. D. Glendening, J. K. Badenhoop, A. E. Reed, J. E. Carpenter, J. A. Bohmann, C. M. Morales, C. R. Landis, F. Weinhold, Theoretical Chemistry Institute, University of Wisconsin, Madison, WI, 2013. <http://nbo6.chem.wisc.edu/>.